PRAMANA
— journal of
physics

Vol. 65, No. 6
December 2005
pp. 1097–1108

Investigation of W/O microemulsion droplets by contrast variation light scattering

ANUJ SHUKLA[1,2,*] and REINHARD H H NEUBERT[1]
[1]Department of Pharmacy, Institute of Pharmaceutics and Biopharmaceutics, Martin-Luther-University Halle-Wittenberg, D-06120 Halle/Saale, Germany
[2]Present address: Lehrstuhl für Physikalische Chemie II Universität Dortmund, Otto-Hahn-Str. 6 D-44227 Dortmund, Germany
*Corresponding author. E-mail: anuj.shukla@uni-dortmund.de

MS received 15 July 2005; accepted 20 August 2005

Abstract. Dynamic and static light scattering experiments have been performed at various molar ratios (μ) of water to AOT and temperatures on water-in-oil (W/O) microemulsions dispersed in n-heptane, n-octane, and n-nonane. Size and shape fluctuations of microemulsion droplets are determined with very high precision because polydispersity influences the characteristic features of scattering data as well as the hydrodynamic radius with μ. Self-consistent interpretation of dynamic and static light scattering data using optical properties and packing consideration on the basis of the layered sphere model are obtained. The estimated extent of polydispersity index of 17% is found, whereas the polydispersity is independent of the alkane types. The geometrical parameters, e.g., hydrodynamic radius, area per head group of the surfactant molecule and thickness of the surfactant layer of microemulsion droplets are also estimated and compared in three different n-alkane types. The best interpretation of the temperature dependence of data has shown a transition from spherical droplets to ellipsoid aggregates with increasing temperature. Axial ratio increases with increase of temperature and the longer the alkane the larger is the axial ratio. The parameters describing the polydispersity and shape change are in agreement with theoretical and experimental results found in the literature.

Keywords. Microemulsions; static and dynamic light scattering.

PACS Nos 68.05; 78.35

1. Introduction

Complex fluids [1] are generally multi-component mixtures. They sometimes possess physical properties of their elements, but in many cases new properties emerge, reflecting the new structural organization of their elements. Multi-component mixtures composed of surfactant, water, and oil have attracted much interest since they form thermodynamically stable phases involving self-organized assemblies. Here we focus on microemulsion, a typical multi-component mixture of three essential components: two immiscible liquids and a surfactant. Typical examples are water-in-oil

or oil-in-water micromulsions. In the former, microdroplets of water (inverse micelles) are dispersed in oil, while in the latter, microdroplets of oil are dispersed in water. Because of many interesting properties involved in the microemulsion systems, considerable efforts (both experimental and theoretical) have been devoted to their studies [2–8]. The rheological properties of the two liquids and the microstructure of phase-separating liquids (size and shape of domains and their spatial distribution) strongly affect the physical properties of the resulting microemulsions. The knowledge of the geometrical parameters of the microemulsion droplets and their size distribution are very important to correctly interpret the observed phenomena and to develop good theoretical models of the driving forces responsible for both droplet formation and solubilization of guest molecules in microemulsions [9].

The W/O microemulsion systems investigated in the present study are the bis(2-ethylhexyl)sulfosuccinate sodium salt (AOT)/water/n-alkanes systems due to it's ability to solubilize [10] large amount of polar solvent (typically water) in apolar solvents without the need for a stabilizing cosurfactant [11]. The microstructure of microemulsions critically depends on the actual system, composition, temperature, and additives [12]. The single-phase W/O microemulsion, we are interested in this study, is normally denoted as L_2 phase. For temperature below 40°C and above 15°C the L_2 microemulsions can be well-represented as a collection of surfactant-coated droplets of water dispersed in a homogeneous medium of oil [13]. The size of W/O microemulsion droplets is highly dependent on the concentration of each constituent solubilized in microemulsion. However, it is recognized that the aggregate size is dominantly characterized by the $[H_2O]/[AOT]$ molar ratio, defined as μ, rather than by actual concentration [14].

Contrast variation light scattering experiments exploit the fact that, since water and AOT have different dielectric constants for water (ε_w) and AOT (ε_s), the optical contrast of the ME droplets changes with μ. The n-alkanes used for the study have dielectric constants (ε_0) that lie between water and AOT. It is therefore possible to combine water and AOT in such proportions that the average dielectric constant of water plus AOT is the same as that of the n-alkane used. At this point, which is normally referred as the optical matching point (OMP), a minimum in the forward scattering intensity is obtained. If all the droplets in the microemulsion have exactly the same water-to-surfactant ratio, the forward scattering will be zero at the OMP. However, if the droplets are polydisperse they will have different water-to-surfactant ratios and there is no single point where all droplets are matched out. As one expects, polydispersity index can be determined very precisely from contrast variation light scattering data in the vicinity of the OMP. In this paper we also present the diffusion coefficient (size) as a function of temperature. The diffusion coefficient is sensitive to shape changes of the microemulsion droplet. The aim of this work is to obtain consistent and unique information about size growth, shape change and polydispersity of microemulsion droplet by contrast variation light scattering.

2. Materials and equipment

AOT (purity 98%), n-heptane (purity 99+ %), n-octane (purity 99+ %), and n-nonane (purity 99+ %) were purchased from sigma-Aldrich, Germany. Water was

used in bi-distilled quality. The basic microemulsion consists of a ternary mixture of n-alkane oil (n = 7, 8, 9), surfactant (AOT) and water. Chain length of the n-alkane oil has been varied in order to show the dependence of some general features of systems on the chain length of n-alkane. Samples were prepared keeping the water weight percentage constant at 5% and varying μ in the range $5 < \mu < 60$ in order to vary the optical contrast of droplets (optical contrast variation). All samples were analyzed in the single-phase microemulsion, normally denoted as L_2 phase (lower phase separation or solubilization temperature T_l = 22.2°C, 17.3°C and 14.5°C and upper phase separation temperature T_u = 62.4°C, 55.3°C and 47.3°C for microemulsion droplets in n-heptane, n-octane and n-nonane respectively) [13,15]. Refractive indices n (optical dielectric constant $\varepsilon = n^2$), molecular volumes v and mass densities ρ at temperature 25°C used for the sample preparation as well as for the mathematical modeling of the ME systems are given in table 1 (in the subsequent formula, subscripts s, w and oil respectively refer to surfactant (AOT), water and n-alkanes). For this work, curvature-dependent area per AOT molecule a_s at the interface is used [6].

$$a_s(\text{Å}^2) = a_0 - 11 \exp[-0.0963(\mu - 10)], \tag{1}$$

where a_0 is a curvature-independent area per AOT molecule in different solvents. Prior to the measurements the samples were filtered through 0.45 μm pore size filter into dust-free sample cells. The cylindrical sample cells are made of Suprasil® quartz glass by Hellma, Muellheim, Germany and have a diameter of 10 mm.

Static and dynamic light scattering experiments were performed on a standard commercial apparatus (ALV) using a green Nd:YAG DPSS-200 mW laser emitting vertically polarized light of wavelength 532 nm. The thermostated sample cell is placed on a motor-driven precision goniometer (±0.01°) which enables the photomultiplier detector to be moved from 20° to 150° scattering angle. The intensity time-correlation functions (ITCF) $g_2(\tau)$ are recorded with an ALV-5000E multiple tau digital correlator with fast option. The minimal sampling time of this correlator is 12.5 ns. For each sample, measurements (the average scattered intensity and the ITCF) were performed at different scattering angles between 50°, 55° and 60°. The average scattered intensity and the ITCF corresponding to one set of experimental parameters have been measured five times and data used for fitting are averaged over these five measurements. In all cases the decay of $g_2(\tau) - 1$ was followed up

Table 1. Refractive indices (n), mass densities (ρ), and molecular volumes (v).

	n	ρ (g/cm^3)	v (Å^3)
AOT	1.4850	1.127	648
H_2O	1.3280	0.997	29.9
n-heptane	1.3851	0.683	–
n-octane	1.3951	0.703	–
n-nonane	1.4050	0.718	–

– Parameter not used.

to values of τ large enough to reach the base line. Temperature of all the measurements was controlled $\pm 0.1^{\circ}$C by a single thermostat with circulating water as the medium. To determine the quality of optical adjustment, test measurements were carried out with pure toluene as a scattering medium showing no angle dependence of the scattering intensity. During the whole measurement period the angle dependence of scattered light intensity was less than 3%. The refractive indices of all samples were measured using a commercial refractometer at a temperature $T \pm 0.2^{\circ}$C.

3. Results and discussion

A. *Layered sphere model*

For the interpretation of our results, a model for microemulsion droplet is needed. A ME droplet modeled as a layered dielectric sphere [16], is considered as made of a water core of radius R_{core}, surrounded by a penetrable shell of thickness L consisting of nonpolar tails of the AOT molecules. The hydrodynamic radius is thus

$$R_{\mathrm{h}} = R_{\mathrm{core}} + L. \tag{2}$$

The AOT is assumed to be entirely at the interface with only a negligible concentration of free molecules in the oil phase. Therefore, the volume fraction (ϕ) of the ME droplets can be defined as $\phi = \phi_{\mathrm{w}} + \phi_{\mathrm{AOT}}$. For layered sphere model, excess polarizability α can be obtained as [17]

$$\alpha = 4\pi\varepsilon_0[E_{\mathrm{w}}R_{\mathrm{core}}^3 + E_{\mathrm{s}}3\frac{\nu_{\mathrm{s}}}{a_{\mathrm{s}}}R_{\mathrm{core}}^2] \tag{3}$$

with reduced dielectric constant $E_i = (\varepsilon_i - \varepsilon_{\mathrm{solvent}})/(\varepsilon_i + 2\varepsilon_{\mathrm{solvent}})$, v_{s} is the specific volume of the surfactant molecule and a_{s} is the average area occupied by a surfactant molecule on the interface.

Figure 1 shows excess polarizability α as a function of μ. It can be seen from figure 1 that for a particular composition of water and AOT, the resulting excess polarizability goes through zero. Figure 1 also shows that the location of this OMP (i.e., $\alpha = 0$) can be shifted by changing the solvent in the ME because of the strong dependence of α on the dielectric constant of solvent ε_0 low ε_0 value leads to a OMP at high μ; see figure 1). We have chosen three n-alkanes ($n = 7$, 8, and 9).

We proceed now comparing the theoretical prediction of the model with the refractive index increment. Refractive index increment Δn of the suspension with respect to the pure oil is related to the average excess polarizability $\langle\alpha\rangle$ as [17]

$$\frac{\Delta n}{\Delta\phi} = \frac{1}{2\sqrt{\varepsilon_{\mathrm{oil}}}}\frac{\langle\alpha\rangle_{\mathrm{excess}}}{\langle\nu_{\mathrm{d}}\rangle} = \frac{W}{2\sqrt{\varepsilon_0}}\frac{(\mu/y)+\nu}{(\mu/y)+1} \tag{4}$$

with

$$w = 3\varepsilon_{\mathrm{oil}}E_{\mathrm{w}}, \quad \nu = \frac{E_{\mathrm{s}}}{E_{\mathrm{w}}} \quad \text{and} \quad y = \frac{\nu_{\mathrm{s}}}{\nu_{\mathrm{w}}}.$$

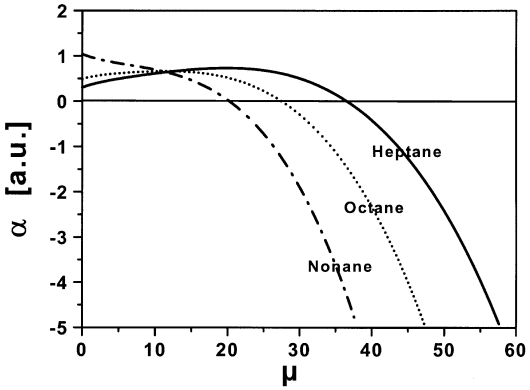

Figure 1. Molar ratio $\mu = [H_2O]/[AOT]$ dependence of the optical excess polarizability α of O/W microemulsion droplet in the systems. Water/AOT/n-alkane from eq. (4).

Note that all the quantities involved in eq. (4) for layered sphere model can be determined from independent measurements. Experimental data are fitted with different values of parameters v_s (548, 648, and 748 Å) because of large range of v_s values reported in the literature [18]. As shown in figure 2, the agreement between the values theoretically predicted by eq. (4) with $v_s = 648$ Å^3 (shown by solid lines) and experimentally measured values is very good. In particular, the predicted OMP, i.e., $(\Delta n/\Delta\phi) = 0$, are close to the experimentally observed OMP. $v_s = 648$ Å^3 is the same as used in ref. [19]. The layered sphere model can thus be used with confidence.

B. *Dynamic light scattering*

ITCF was fitted by second-order cumulants method [20]. First a single exponential was used to fit the base line because the second cumulant (Γ_2) is very sensitive to the correct value of the baseline (A_0). Then A_0 estimate was subtracted from the data, logarithms of these data are plotted as a function of the delay time τ and it was refit by a polynomial from which first cumulant (Γ_1) and second cumulant (Γ_2) were extracted [3]. The apparent diffusion coefficient D_{app} has been deduced from Γ_1. Polydispersity, $\gamma = (\langle R^2\rangle - \langle R\rangle^2)/\langle R\rangle^2$ calculated from Γ_2 was for all samples $\sim$0.10. To get the free diffusion coefficients (D_0) of the droplets, D_{app} is corrected for interaction potential [2]. If D_0 is known, the mean hydrodynamic radius $\langle R_h\rangle$ can be obtained from Stokes–Einstein equation

$$\langle R_h\rangle = \frac{k_B T}{6\pi\eta D_0} = \frac{\langle\alpha^2\rangle}{\langle\alpha^2/R_h\rangle}, \tag{5}$$

where k_B is the Boltzmann's constant, T is the absolute temperature and η is the coefficient of viscosity of the solvent (the continuous phase in the case of ME). Initial studies indicated that the MEs were too small to exhibit significant angular

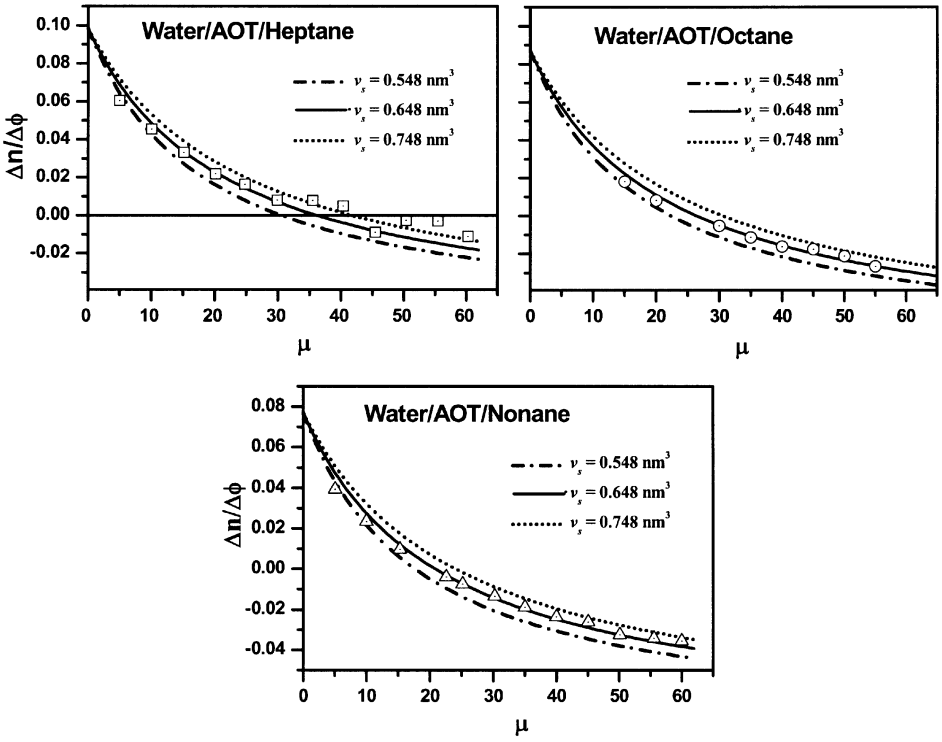

Figure 2. Experimental data points for the refractive index of microemulsion droplet as a function of μ at temperature 25°C. The theoretical prediction by eq. (6) is shown as solid line.

dependence. Therefore, results used for the discussion are the average of the results obtained at three different angles. Mean hydrodynamic radius $\langle R_\mathrm{h} \rangle$ as a function of molar water-to-AOT ratio μ is plotted in figures 3b–d. Sigmodial shape of $\langle R_\mathrm{h} \rangle$ in the vicinity of OMP vs. μ reflects the polydispersity of MEs [21]. Position of the OMP and sigmoidal shape of $\langle R_\mathrm{h} \rangle$ can be fitted using only two adjustable parameters γ and a_0 [17]. As shown in figure 3a, a change of the parameter a_0 results merely in a vertical shift of the fitting curve. The sigmoidal shape of $\langle R_\mathrm{h} \rangle$, which is the characteristic shape of polydisperse MEs is thus given by a single parameter γ. A reasonable fit of our experimental data can be obtained with a_0 and γ as shown in figures 3b–d and listed in table 2. Best fitted value leads to OMP at $\mu \sim 35$, 25 and 20 for droplets in n-heptane, n-octane and n-nonane respectively as expected from figure 2. These results are consistent with $\langle R_\mathrm{h} \rangle$ varies linearly with μ (except in the vicinity of OMP) are shown by an array of different techniques [22–26]. Further, as shown in figure 3b–d, linear dependence of R_h on μ greater than the value for OMP are fitted according to the linear eq. (1). This yields the thickness of surfactant layer L from the intercept.

Table 2. Results (polydispersity index γ optical matching point (OMP) and area per head group at interface a_0) obtained from DLS and SLS.

	DLS				SLS	
	γ	OMP	a_0 (Å^2)	$\langle$L$\rangle$ (Å)	γ	OMP
Water/AOT/n-heptane	0.03	35	56	22.7	0.03	35
Water/AOT/n-octane	0.03	25	50	25.6	0.03	25
Water/AOT/n-nonane	0.03	20	46	25.0	0.03	20

C. *Static light scattering*

A similar effect as obtained for $\langle R_\mathrm{h}\rangle$ can be observed in the dependence of the normalized intensity $\langle I_\mathrm{s}\rangle$ on μ. As shown in figure 4a, normalized intensity goes through zero for monodisperse systems at the OMP. However, if the droplets are polydisperse, in the vicinity of OMP the scattering intensity exhibits a sharp dip but there remains a substantial residual scattering. The depth and position of the characteristic dip of the normalized scattering intensity at the optical matching can be fitted with only one free parameter γ [17]. A reasonable fit of experimental data can be obtained with γ shown in figures 4b–d and listed in table 2. The values for γ are in agreement with the values obtained from DLS.

The fact that one can obtain a self-consistent interpretation of SLS and DLS data on the basis of the layered polydisperse sphere model – both sets of data resulting from fundamentally different measurements – confirm the small polydispersity index $\sigma_\mathrm{s} = \sqrt{\gamma} = 0.17$ of the droplet radius in MEs and independent of n-alkane chain. It has been predicted theoretically from multiple chemical equilibrium approach [27,28] that the size of the polydispersities σ_s in the range of 0.1 to 0.25 are independent of the alkane type [29–31]. These values are also consistent with the value $\sigma_\mathrm{s} = 0.16$ obtained from careful analysis of SANS data in the full $\vec{q}$ range for D_2O/AOT/decane and D_2O/AOT/iso-octane by Arleth *et al* [19]. Polydispersity index $\sigma_\mathrm{s} = 0.32$ obtained from second-order cumulant fitting is substantially higher than the value obtained from contrast variation experiments. As already pointed out by several authors [9,32] the second cumulant (represents only small correction to the shape of the correlation function) overestimates the polydispersity of microemulsion droplets.

We note that area per AOT head group decreases as the alkane chain length increases (see table 2). The possible explanation for this is that R_h is slightly larger in the larger chain alkane oil because oil penetration into the surfactant tail region is smaller, which causes decrease in spontaneous curvature of the surfactant layer in comparison to smaller chain. Small droplets have larger area per volume than the large droplet. This implies that area per AOT head group decreases with increase of chain length. The values for thickness of the surfactant layer $\langle L\rangle$ (see table 2) are somewhat higher than the value estimated for hydrophobic chain length of the surfactant (AOT) $L = 9$ Å. This deviation could be explained by assuming the existence of several layers of solvent molecules, which migrate with the droplet.

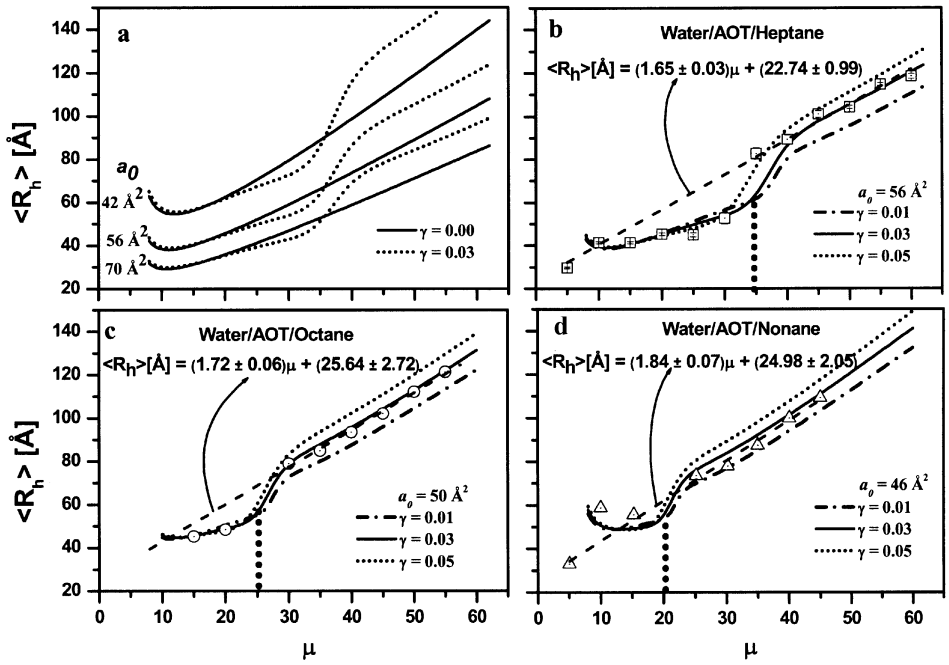

Figure 3. Average hydrodynamic radius $\langle R_\mathrm{h}\rangle$ of ME droplet as a function of μ at temperature 25°C. Prediction of $\langle R_\mathrm{h}\rangle$ by eq. (2) for three different values of a_0 are shown in (**a**). Three fits of experimental data by eq. (2) are shown in (**b**) water/AOT/n-heptane, (**c**) water/AOT/n-octane and (**d**) water/AOT/n-nonane.

D. *Shape fluctuations*

For the MEs measured as a function of temperature, μ was fixed as 60 for water/AOT/n-heptane, 45 for water/AOT/n-octane and 30 for water/AOT/n-nonane systems. Due to the small droplet size and the low polydispersity ($\sigma_\mathrm{s} \sim 0.17$) the scattering intensity near the OMP is very low, which lead unfavorable signal-to-noise ratio. Therefore μ values are chosen far from OMP to get sufficient intensity. Temperature in the range 25°C $< \alpha <$ 37.5°C (temperature has been varied in the region of the phase diagram where surfactant covered water droplets are formed) has been varied in order to show the effect of temperature on the shape of the droplets.

Mean hydrodynamic radius $\langle R_\mathrm{h}\rangle$ versus normalized temperatures (T/η) are plotted in figures 5a–c. In the systems where no structural changes occur, the radii should be independent of the temperature, as predicted by the Stokes–Einstein eq. (5). As shown in figures 5a–c, for MEs investigated, this is clearly not fulfilled. This observation is consistent with the results obtained for AOT/water/n-alkane system using time-resolved luminescence quenching techniques [13] and for the $C_{12}E_5$/water/decane system using nuclear magnetic resonance (NMR) techniques [33,34] and for AOT/water/isooctane system using small angle X-ray scattering [35]

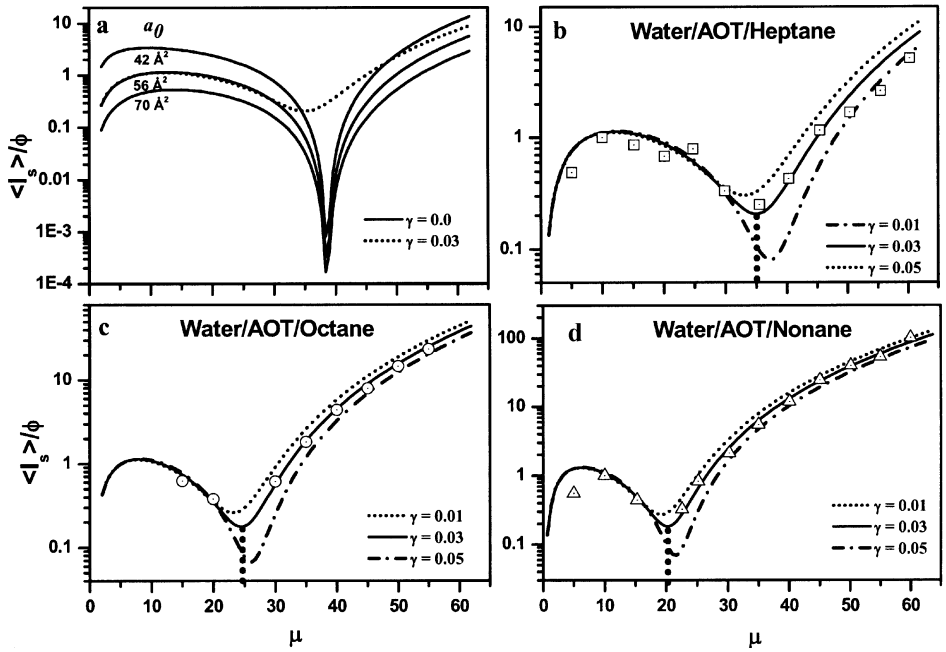

Figure 4. Normalized scattering intensity $\langle I_s \rangle/\phi$ of ME droplet as a function of μ at temperature 25°C. Prediction of $\langle I_s \rangle/\phi$ by eq. (1) for three different values of a_0 are shown in (**a**). Three fits of experimental data by eq. (1) are shown in (**b**) water/AOT/n-heptane, (**c**) water/AOT/n-octane, and (**d**) water/AOT/n-nonane.

that with increase of temperature aggregation takes place in the direction of vanishing spontaneous curvature, leading to structural change from spherical droplet to ellipsoid. For such a case, diffusion coefficient of the MEs at infinite dilution can be obtained, by attaching a correction term concerning shape, to the Stokes–Einstein and Perrin equations [36]. Using the constant-area-to-enclosed-volume constraint, one can write expression for diffusion coefficient of the prolate and oblate MEs at infinite dilution as [34]

$$D^0_{\text{prolate}} = \frac{k_B T}{6\pi\eta R} \frac{2\ln\left(\rho + \sqrt{\rho^2 - 1}\right)}{\sqrt{(\rho^2 - 1/\rho^2)} + \rho \arccos(1/\rho)}, \tag{6}$$

$$D^0_{\text{oblate}} = \frac{k_B T}{6\pi\eta R} \frac{2\arctan\left(\sqrt{\rho^2 - 1}\right)}{\sqrt{(\rho^2 - 1)} + \arccos h(\rho)/\rho}, \tag{7}$$

where R is the radius of the sphere and ρ is the axial ratio ($\rho = a/b$ with a being the length of the long axis and b being the length of the short axis).

It is interesting that at temperatures up to 10°C above the lower solubilization temperatures T_1 of microemulsion droplets in n-alkanes, nearly no change in the

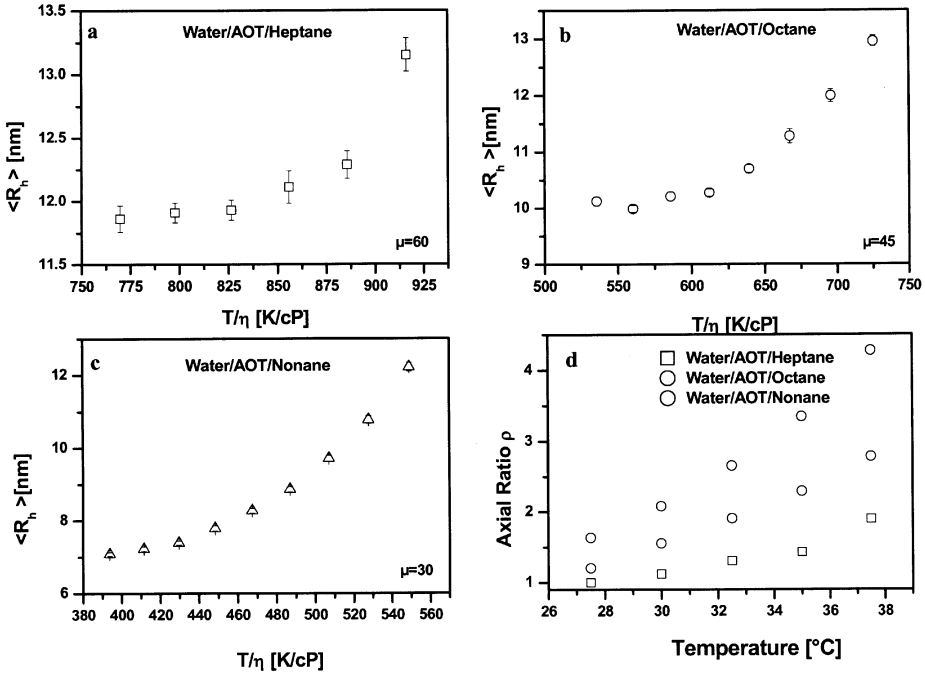

Figure 5. T/η dependence of the mean hydrodynamic radius $\langle R_{\rm h}\rangle$ of the ME droplets: (**a**) water/AOT/heptane, (**b**) water/AOT/octane, (**c**) water/AOT/nonane. (**d**) Average axial ratios as a function of temperature.

radius occur. Therefore, assuming the ME droplets to grow from spheres at 25°C to spheroids, it is possible to calculate the axial ratios from the diffusion coefficient using eqs (6) and (7). No significant difference between the prolate and oblate models is obtained. Figure 5d shows only prolates axial ratio as a function of temperature. It has been concluded that prior to the upper two-phase boundary temperature $T_{\rm u}$ the growth of MEs is limited to an axial ratio as shown in figure 5d. Axial ratio increases with increase of temperature and the longer the alkane chain the larger is the axial ratio. An increase of size polydispersity with temperature found by Kotlarchyk *et al* [26] may be attributed to the shape fluctuations of the droplet from spherical to aspheric. This temperature and alkane chain length dependence of the shape of the droplets can be explained by the temperature and alkane chain length dependence of the spontaneous curvature of surfactant film. Increasing the temperature above the lower solubilization temperature favors less negative spontaneous curvature (surfactant polar head groups on the interior of the aggregate and the apolar tails on the exterior surface, define here as negative curvature) and often observed near the phase inversion temperature, ME has a bicontinuous structure with zero net surfactant film curvature. It is known that due to reduced solubility of the surfactant in longer-chain [37], longer chain-length alkane oils shift solubilization temperature to lower temperatures. Therefore at constant temperature, longer the alkane chain the smaller will be the negative curvature hence larger the axial ratio.

4. Conclusion

Molar water-to-AOT ratio (μ) dependence of droplet size of AOT W/O microemulsions in three different solvents was investigated using light scattering. The polydispersity index γ of the microemulsion droplets are determined and compared in three different n-alkanes. For AOT microemulsions in heptane, octane and nonane, we found $\gamma \sim 0.03$. The geometrical parameters, e.g., hydrodynamic radius, area per head group of the surfactant molecule and thickness of the surfactant layer of microemulsion droplets are estimated and compared in three different n-alkanes. It is observed that area per head group for fixed composition decreases as the alkane chain length increases. The result that microemulsion droplets in short chain alkane oil are slightly smaller in comparison to droplets in larger chain alkane oil is consistent with the penetrable layered sphere model. Self consistent interpretations of both dynamic and static light scattering data were obtained using optical properties and packing consideration on the basis of the layered sphere model. Shape changes of ME droplets with increase of temperature were determined and compared in three different n-alkane types. The parameter (axial ratio ρ) describing shape change was evaluated. It was observed that at temperatures up to 10°C above the lower solubilization temperatures of W/O MEs, nearly no change in the shape of the droplet occur. Axial ratio increases with increase of temperature and the longer the alkane chain the larger is the axial ratio. The parameters describing the polydispersity and shape change are in agreement with parameters determined earlier for MEs stabilized by AOT using SAXS [35], NMR [33], and combination of SANS and NSE [30].

Acknowledgement

Financial support by the Deutsche Forschungsgemeinschaft (GK 134) and the Institute for Applied Dermatopharmacy at the Martin Luther University Halle-Wittenberg e.V. is gratefully acknowledged.

References

[1] P G de Gennes and J Prost, *Physics of liquid crystals* (Clarendon, Oxford, 1993)
[2] A Shukla, H Graener and R H H Neubert, *Langmuir* **20**, 8526 (2004)
[3] A Shukla, A Krause and R H H Neubert, *J. Pharmacy and Pharmacology* **55**, 741 (2003)
[4] A Shukla, M Janich, K Jahn and R H H Neubert, *J. Pharm. Sci.* **92**, 730 (2003)
[5] A Shukla, M Janich, K Jahn, A Krause, M A Kiselev and R H H Neubert, *Pharm. Res.* **19**, 881 (2002)
[6] E B Leodidis, T A Hatton in *Structure and reactivity of reverse micelles* edited by M P Pileni (Elsevier Science, Amsterdam, 1989) vol. 65, p. 270
[7] P L Luisi and L Magid, *J. CRC Crit. Biochem.* **20**, 409 (1986)
[8] M Malmsten, Microemulsions, in: *Handbook of microemulsion science and technology pharmaceuticals* edited by P Kumar and K L Mittal (Marcel Dekker, New York, 1999) p. 755

V Pillai, J R Kanicky and D O Shah, in *Handbook of microemulsion science and technology pharmaceuticals* edited by P Kumar and K L Mittal (Marcel Dekker, New York, 1999) p. 743
[9] S Christ and P Schurtenberger, *J. Phys. Chem.* **98**, 12708 (1994)
[10] S A Lossia, S G Flore, S Nimmala, H Li and S J Schlick, *J. Phys. Chem.* **96**, 6071 (1992)
[11] L M M Nazario, T A Hatton and J P S G Crespo, *Langmuir* **12**, 6326 (1996)
[12] S H Chen, J Rouch, F Sciortino and P Targagilia, *J. Phys.: Condens. Matter* **6**, 10855 (1994)
[13] H Mays and G Ilgenfritz, *J. Chem. Soc., Faraday Trans.* **92**, 3145 (1996)
[14] B H Robinson, C Toprakcioglu, J C Dore and P Chieux, *J. Chem. Soc., Faraday Trans. I* **80**, 13 (1984)
[15] J Rouch, A Safouane, P Tartaglia and S H Chen, *J. Chem. Phys.* **90**, 3756 (1989)
[16] J S Huang, M Kotlarchyk and S H Chen, in *Micellar solutions and MEs: Structure, dynamics and statistical thermodynamics* edited by S H Chen and R Rajagopalan (Spinger, New York, 1990)
[17] J Ricka, M Borkovec and U Hofmeier, *J. Chem. Phys.* **94**, 8503 (1991)
[18] T Patzlaff, Pikosekunden-Infrarotspektroskopie der ultraschnellen Abkühlung nanoskopischer Wassertropfen in Mikroemulsionen, PhD Dissertation (Martin-Luther-University, Halle/Saale, Germany, 2002)
[19] L Arleth and J S Pedersen, *Phys. Rev.* **E63**, 061406-1 (2001)
[20] D E J Koppel, *J. Chem. Phys.* **57**, 4814 (1972)
[21] A Shukla, Characterization of microemulsions using small angle scattering techniques, PhD Dissertation (Martin-Luther-University, Halle/Saale, Germany, 2003)
[22] I D Charlton and A P Doherty, *J. Phys. Chem.* **104**, 8061 (2000)
[23] A J W G Visser, K Vos, A van Hoek and J S Santema, *J. Phys. Chem.* **92**, 759 (1988)
[24] J Eastoe, B H Robinson, A J W G Visser and D C Steytler, *J. Chem. Soc. Faraday Trans.* **87**, 1899 (1991)
[25] M Kotlarchyk, R B Stephens and J S Huang, *J. Phys. Chem.* **92**, 1533 (1988)
[26] M Kotlarchyk, S H Chen and J S Huang, *J. Phys. Chem.* **86**, 3273 (1982)
[27] J C Eriksson and S Ljunggren, *Prog. Colloid Polym. Sci.* **81**, 41 (1990)
[28] J C Eriksson and S Ljunggren, *Langmuir* **11**, 1145 (1995)
[29] M Gradzielski, D Langevin and B Farago, *Phys. Rev.* **E53**, 3900 (1996)
[30] T Hellweg, D Langevin, Physica A **264**, 370 (1999)
[31] J Eastoe, L Sharpe, R K Heenan and S Egelhaaf, *J. Phys. Chem.* **B101**, 904 (1997)
[32] Y D Yan and J H R Clarke, *J. Chem. Phys.* **93**, 4501 (1990)
[33] M S Leaver, U Olsson, H Wennerström and R Strey, *J. Phys. II* **4**, 515 (1994)
[34] M S Leaver, I Furo and U Olsson, *Langmuir* **11**, 1524 (1995)
[35] D I Svergun, P V Konarev, V V Volkov, M H Koch, W F C Sager, J Smeets and E M Blokhuis, *J. Chem. Phys.* **113**, 1651 (2000)
[36] P C Heimenz, *Principles of colloid and surface chemistry* (New York: Marcel Dekker Inc., 1984)
[37] M Kahlweit, R Strey and G Busse, *J. Phys. Chem.* **94**, 3881 (1990)